ROBUST AND EFFICIENT SOLUTION OF THE DRUM PROBLEM VIA NYSTRÖM APPROXIMATION OF THE FREDHOLM DETERMINANT

LIN ZHAO AND ALEX BARNETT

ABSTRACT. The "drum problem"—finding the eigenvalues and eigenfunctions of the Laplacian with Dirichlet boundary condition—has many applications, yet remains challenging for general domains when high accuracy or high frequency is needed. Boundary integral equations are appealing for large-scale problems, yet certain difficulties have limited their use. We introduce two ideas to remedy this: 1) We solve the resulting nonlinear eigenvalue problem using Boyd's method for analytic root-finding applied to the Fredholm determinant. We show that this is many times faster than the usual iterative minimization of a singular value. 2) We fix the problem of spurious *exterior resonances* via a combined-field representation. This also provides the first robust boundary integral eigenvalue method for non-simply-connected domains. We implement the new method in two dimensions using spectrally accurate Nyström product quadrature. We prove exponential convergence of the determinant at roots for domains with analytic boundary. We demonstrate 13-digit accuracy, and improved efficiency, in a variety of domain shapes including a non-convex cavity shape with strong exterior resonances.

1. INTRODUCTION

Eigenvalue problems (EVPs) for linear PDEs have a wealth of applications [6] to modeling vibration problems, acoustic, electromagnetic and quantum cavity resonances, as well as in modern areas such as nano-scale devices [37], micro-optical resonators for high-power lasers [44], accelerator design [1], and data analysis [40]. The paradigm is the Dirichlet eigenvalue problem: given a bounded connected domain $\Omega \subset \mathbb{R}^2$ with boundary Γ, to find eigenvalues κ^2 and corresponding nontrivial eigenfunctions u that satisfy

$$(\Delta + \kappa^2)u = 0 \qquad \text{in } \Omega, \tag{1}$$

$$u = 0 \qquad \text{on } \Gamma, \tag{2}$$

where $\Delta := \partial^2/\partial x_1^2 + \partial^2/\partial x_2^2$ is the Laplacian. We refer to κ as the eigenfrequency, and label the allowable set $\kappa_1 < \kappa_2 \leq \kappa_3 \leq \cdots \nearrow +\infty$, counting multiplicities. u_j will refer to an eigenfunction (also known as an eigenmode) for the eigenfrequency κ_j. A numerical solution is necessary in all but a few special shapes (in 2D, ellipses and rectangles) where the Laplacian is separable [22]. This and related EVPs are also of interest in mathematical areas such as quantum chaos [38]. This is covered in excellent reviews by Kuttler–Sigillito [34] and Grebenkov–Nguyen [26].

Numerical solution methods for (1)–(2) fall broadly into two categories: A) direct discretization, using finite differencing or finite elements to give a sparse linear EVP where κ^2 is the eigenvalue; vs B) reformulation as a boundary integral equation (BIE) [8] discretized using the Galerkin or Nyström methods, or as boundary collocation of particular solutions [17], resulting in a highly *nonlinear* EVP, again for the eigenvalue κ^2 or eigenfrequency κ. The nonlinearity with respect to κ comes from that of the fundamental solution to the Helmholtz equation (1). The advantages of

Date: May 2, 2015.

type B include: a huge reduction in the number of unknowns (due to the decrease in dimensionality by one) especially at high frequency, and increased accuracy (since finite element high-frequency "pollution" [7] is absent). At least in two dimensions (2D), spectrally-accurate BIE quadratures exist for smooth domains [32, 13], and for corners and Dirichlet-Neumann junctions [32, 2]. Yet, as pointed out by Bäcker [8, Sec. 3.3.6], the standard BIE method is not even robust for a simply-connected domain, due to the possibility of spurious exterior resonances. Recently, type-B methods which approximately *linearize* the nonlinearity, hence boost efficiency at high frequency, have been created, but these are limited to moderate κ [29], to heuristic methods with low accuracy [43, 45], or to domains that are star-shaped [46, 9, 10, 13]. This motivates the need for a robust type-B method that applies to all domain shapes, including multiply-connected ones, and remains efficient up to at least medium-high frequencies.

In this work we solve two of these issues: (1) The standard approach to solve the nonlinear EVP is by searching for "V-shaped" minima of a smallest singular value [42]; we boost efficiency by turning this into a search for the roots of a function that is *analytic* (in a large region of the complex plane; see Remark 9.2), which can be done with less function evaluations and also without the expensive computation of the SVD. (2) We cure the exterior resonance problem, and at the same time handle multiply-connected domains, using a combined field integral equation (54). We also provide several analysis results that place our method on a rigorous footing.

The outline of this paper is as follows. In Section 2 we review the use of potential theory to reformulate the eigenvalue problem as a BIE, and give a discretization of the BIE due to Kress [32] that achieves spectral accuracy for smooth domains. To tackle issue (1) above, in Section 3 we introduce the *Fredholm determinant*,

$$f(\kappa) = \det(I - 2D(\kappa)) \;, \tag{3}$$

where D is the double-layer operator (defined by (8) below), whose roots are precisely the eigenfrequencies κ_j for simply connected domains. Following Bornemann [18], we approximate this with the determinant of a Nyström matrix. Our main Theorem 4.3, in Section 4, states that this approximation convergences exponentially to zero at the true eigenfrequencies, if the domain has analytic boundary. Since $f(\kappa)$ is analytic for nonzero κ, we propose in Section 5 applying Boyd's method to find its roots, an application we have not seen in the literature before. In Section 7 we prove, and demonstrate numerically, that the CFIE (54) is robust on the real axis for domains with interior holes. It is well known that finding roots becomes ill-conditioned when they are close, hence we explain in Section 8 how we retain robustness in the case of nearby eigenvalues by reverting to the (more expensive) SVD method in these (rare) case. Section 10 gives numerical performance tests of the entire scheme, achieving 13 digits the first 100 eigenfrequencies of a generic smooth domain, and a domain with exterior resonances, showing that our method is competitive in terms of both accuracy and timing.

2. Boundary integral formulation and quadrature scheme

Now we lay the foundation of our method for computing eigenfrequencies by describing the boundary integral formulation and its analyticity properties for analytic domains, and then its numerical treatment in 2D, which is standard.

2.1. **Integral equation formulation.**

For a bounded domain Ω with twice continuously differentiable boundary Γ, we explicitly construct solutions to the Helmholtz equation by layer potentials

using the fundamental solution. The fundamental solution is given by

$$\Phi(x,y) := \frac{i}{4}H_0^{(1)}(\kappa|x-y|), \quad x \neq y, \quad x,y \in \mathbb{R}^2, \tag{4}$$

where $H_0^{(1)}$ is the first-kind Hankel function of order zero.

For a continuous function φ on Γ, the single layer operator $\mathcal{S} : C(\Gamma) \to C(\mathbb{R}^2\backslash\Gamma)$ is defined as follows, with v denoting the resulting single layer potential

$$v(x) = \mathcal{S}\varphi(x) := \int_\Gamma \Phi(x,y)\varphi(y)ds(y), \quad x \in \mathbb{R}^2\backslash\Gamma, \tag{5}$$

where $ds(y)$ is the arc-length element on Γ. Note that the domain of v excludes Γ. The corresponding single layer boundary operator $S : C(\Gamma) \to C(\Gamma)$ is

$$S\varphi(x) := \int_\Gamma \Phi(x,y)\varphi(y)ds(y), \quad x \in \Gamma. \tag{6}$$

The double layer operator $\mathcal{D} : C(\Gamma) \to C(\mathbb{R}^2\backslash\Gamma)$ with the associated double layer potential denoted by u is defined as

$$u(x) = \mathcal{D}\varphi(x) := \int_\Gamma \frac{\partial\Phi(x,y)}{\partial n(y)}\varphi(y)ds(y), \quad x \in \mathbb{R}^2\backslash\Gamma, \tag{7}$$

where $n(y)$ is the unit normal vector at $y \in \Gamma$ directed to the exterior of the domain. Because the integral exists in the principal value sense for $x \in \Gamma$, one may define a double layer boundary operator $D : C(\Gamma) \to C(\Gamma)$ by

$$D\varphi(x) := \int_\Gamma \frac{\partial\Phi(x,y)}{\partial n(y)}\varphi(y)ds(y), \quad x \in \Gamma. \tag{8}$$

The above operators depend on the frequency κ, and we will indicate this only when needed.

Both u and v as defined are solutions to the Helmholtz equation. Both u and its normal derivative u_n can be continuously extended, either from the interior or the exterior of Ω, to the boundary Γ by taking limits in the following sense:

$$u^\pm(x) := \lim_{h\to 0+} u(x \pm hn(x)), \qquad u_n^\pm(x) := \lim_{h\to 0+} n(x)\cdot\nabla u(x \pm hn(x)), \qquad x \in \Gamma. \tag{9}$$

Extensions to the boundary can be done for v and v_n in the same way as above. These limits relate to the boundary operators via the jump relations [21]

$$v^\pm(x) = S\varphi(x), \qquad x \in \Gamma, \tag{10}$$

$$v_n^\pm(x) = (D^T \mp \tfrac{1}{2})\varphi(x), \quad x \in \Gamma, \tag{11}$$

$$u^\pm(x) = (D \pm \tfrac{1}{2})\varphi(x), \quad x \in \Gamma, \tag{12}$$

$$u_n^\pm(x) = T\varphi(x), \qquad x \in \Gamma, \tag{13}$$

where D^T is given by

$$D^T\varphi(x) := \int_\Gamma \frac{\partial\Phi(x,y)}{\partial n(x)}\varphi(y)ds(y), \quad x \in \Gamma, \tag{14}$$

and the hypersingular operator T is defined by

$$T\varphi(x) := \frac{\partial}{\partial n(x)}\int_\Gamma \frac{\partial\Phi(x,y)}{\partial n(y)}\varphi(y)ds(y), \quad x \in \Gamma. \tag{15}$$

When u is given by a double layer potential with density φ, enforcing the Dirichlet boundary condition (2) gives

$$(I - 2D(\kappa))\varphi = 0. \tag{16}$$

Thus we might hope that the (nonlinear) eigenvalue problem that $I-2D(\kappa)$ has a nontrivial nullspace is equivalent to the (linear) eigenvalue problem (1)–(2). For a domain of general connectivity there is *not* such an equivalence; we merely have the following.

Lemma 2.1. *Let Ω be a (possibly non-simply connected) bounded domain with twice continuously differentiable boundary Γ. Then if κ^2 is a Dirichlet eigenvalue of Ω, $I - 2D(\kappa)$ has a nontrivial nullspace.*

Proof. Green's representation formula [21, Theorem 2.1] states that if $(\Delta + \kappa^2)u = 0$ in Ω, then

$$\mathcal{S}u_n^- - \mathcal{D}u^- = \begin{cases} u, & \text{in } \Omega, \\ 0, & \text{in } \mathbb{R}^2 \backslash \overline{\Omega}. \end{cases} \tag{17}$$

Applying this to u an eigenfunction with eigenfrequency κ_j, and taking its derivative on Γ using (11) gives $u_n^- = (D^T + \frac{1}{2})u_n^-$. Since u_n^- is nontrivial, the compactness of D and the Fredholm alternative proves $I - 2D(\kappa_j)$ has a nontrivial nullspace. □

The consequence for a multiply-connected domain is that it is possible that there are *spurious* frequencies where $I - 2D(\kappa)$ has a nontrivial nullspace but κ^2 is not a Dirichlet eigenvalue (we will characterize these frequencies in Lemma 7.1).

Only for the case of Ω simply-connected does equivalence hold, as the following well-known theorem states.

Theorem 2.2. [20] *Let Ω be a bounded, simply-connected domain with twice continuously differentiable boundary Γ. Then for each $\kappa \in \mathbb{C}\backslash\{0\}$ with $\operatorname{Im}\kappa \geq 0$, κ^2 is a Dirichlet eigenvalue of Ω if and only if $I - 2D(\kappa)$ has a nontrivial nullspace. Moreover, the dimension of the eigenspace is the same as that of the nullspace.*

For the case of Lipschitz (ie non-smooth) boundary, see Mitrea [36]. This motivates integral equations as a robust approach to the Dirichlet eigenvalue problem for simply-connected domains; later in Section 7 we will show how to handle multiply-connected domains.

2.2. **Splitting of the kernel.** We will discuss a quadrature scheme for Helmholtz kernels that is highly accurate for smooth boundaries [32]; for this an analytic splitting is needed. Assume Γ is analytic and has a regular parametrization $x(t) = (x_1(t), x_2(t)), 0 \leq t \leq 2\pi$. We transform (16) into the parametric form

$$\psi(t) - \int_0^{2\pi} L(t,s)\psi(s)ds = 0, \quad 0 \leq t \leq 2\pi, \tag{18}$$

where $\psi(t) := \varphi(x(t))$ and the kernel of the reparametrized operator $2D(\kappa)$ is given by

$$L(t,s) := \frac{\partial \Phi(x(t), x(s))}{\partial n(x(s))} |x'(s)| \tag{19}$$

$$= \frac{i\kappa}{2}\{x_2'(s)[x_1(t) - x_1(s)] - x_1'(s)[x_2(t) - x_2(s)]\}\frac{H_1^{(1)}(\kappa r(t,s))}{r(t,s)}, \tag{20}$$

with the distance function $r(t,s) := \{[x_1(t) - x_1(s)]^2 + [x_2(t) - x_2(s)]^2\}^{\frac{1}{2}}$.

With a slight abuse of notation, at each κ we use $L(\kappa) : C[0, 2\pi] \to C[0, 2\pi]$ to denote the integral operator with $L(t, s)$ as its kernel, that is, the reparametrized operator $2D$. We will sometimes drop the explicit dependence on κ and write L. The kernel $L(t, s)$ is continuous but not analytic, so one splits the kernel into

$$L(t,s) = L^{(1)}(t,s)\ln\big(4\sin^2\frac{t-s}{2}\big) + L^{(2)}(t,s), \tag{21}$$

where

$$L^{(1)}(t,s) := -\frac{\kappa}{2\pi}\{x_2'(s)[x_1(t)-x_1(s)] - x_1'(s)[x_2(t)-x_2(s)]\}\frac{J_1(\kappa r(t,s))}{r(t,s)}, \tag{22}$$

$$L^{(2)}(t,s) := L(t,s) - L^{(1)}(t,s)\ln\big(4\sin^2\frac{t-s}{2}\big). \tag{23}$$

Both $L^{(1)}$ and $L^{(2)}$ are analytic, provided that Γ is analytic [32]. In that case we get the following.

Lemma 2.3. *Let Ω have analytic boundary. Then any density function $\psi(s)$ solving* (18) *is an analytic function of the parameter s.*

This follows from the argument of [33, Prob. 12.4, p. 217], namely that the operator L is compact in the space of 2π-periodic analytic functions in a complex strip $\mathbb{R}\times(-a, a)$ for some $a > 0$, and the Fredholm alternative.

2.3. **Quadrature and Nyström method.** We choose a set of quadrature points equidistant in parameter, $s_k := \frac{2\pi k}{N}$, $k = 0, 1, ..., N-1$, where N is an even number, with equal weights $2\pi/N$, and insert this quadrature into (18) to get the approximation

$$\psi^{(N)}(t) - \sum_{k=0}^{N-1}\{R_k^{(N)}(t)L^{(1)}(t,s_k) + \frac{2\pi}{N}L^{(2)}(t,s_k)\}\psi^{(N)}(s_k) = 0, \quad 0 \le t \le 2\pi. \tag{24}$$

Here the second term inside the curly brackets arises from the usual quadrature rule, whereas the first term arises from a spectrally-accurate product quadrature scheme for the periodized log singularity (reviewed in [28, Sec. 6]), with weights

$$R_k^{(N)}(t) = -\frac{4\pi}{N}\sum_{m=1}^{\frac{N}{2}-1}\frac{1}{m}\cos m(t-s_k) - \frac{4\pi}{N^2}\cos\frac{N}{2}(t-s_k), \quad k = 0, \dots, N-1. \tag{25}$$

Define L_N to be the Nyström interpolant from (24), which maps $\psi \in C[0, 2\pi]$ to

$$L_N\psi(t) = \sum_{k=0}^{N-1}\{R_k^{(N)}(t)L^{(1)}(t,s_k) + \frac{2\pi}{N}L^{(2)}(t,s_k)\}\psi(s_k). \tag{26}$$

Kress [33, Sec. 12.3] showed that, when $L^{(1)}$ and $L^{(2)}$ are analytic, interpolation of analytic functions with this product quadrature convergences exponentially with N in the L_∞-norm. Thus for each analytic ψ, $\|L_N\psi - L\psi\|_\infty \le Ce^{-aN}$ for some constants C and a depending on ψ [33, p. 185].

By setting t to s_i in (26), one obtains the Nyström matrix M_N with elements

$$(M_N)_{ij} := R_{|i-j|}^{(N)}(0)L^{(1)}(s_i,s_j) + \frac{2\pi}{N}L^{(2)}(s_i,s_j), \quad i,j = 0,\dots,N-1. \tag{27}$$

The condition (18) that $I - 2D(\kappa)$, and hence $I - L(\kappa)$, is singular can now be approximated with exponentially small error by the condition that the matrix $I - M_N(\kappa)$ is singular. Each null-vector of $I - L_N$ is exactly reconstructed by applying the interpolant on the right-hand side of (26) to the

corresponding null-vector of the matrix. By the analysis in [33, Sec. 12.2-12.3] in the homogeneous case, this reconstructs the desired null vectors of $I - L$ to exponential accuracy.

3. The Fredholm determinant

As we have seen, for simply-connected domains, κ is an eigenfrequency if and only if the boundary integral operator $I - L(\kappa)$ has a nontrivial nullspace. We now convert this to a condition on the Fredholm determinant.

The following theorem says that we can study the invertibility of $I - L$ on $L_2[0, 2\pi]$ instead of $C[0, 2\pi]$.

Theorem 3.1. [27] [33, p. 91] *Let A be an integral operator with weakly singular kernel, then the nullspaces of $I - A$ in $C[0, 2\pi]$ and $L_2[0, 2\pi]$ coincide.*

This implies that L has the same set of nonzero eigenvalues, counting multiplicities, in $C[0, 2\pi]$ as in $L_2[0, 2\pi]$. Thus from now on we need not specify in which space we consider these eigenvalues.

Now we define *trace class operators*. Let $\mathcal{H}$ be a complex, separable Hilbert space and A a compact linear operator on $\mathcal{H}$ with its adjoint operator denoted by A^*, we can list the nonzero eigenvalues of A^*A, counting multiplicities, as follows

$$\lambda_1(A^*A) \geq \lambda_2(A^*A) \geq \lambda_3(A^*A) \geq ... \searrow 0,$$

and then the singular values $\{\sigma_j\}$ of A are defined as

$$\sigma_j(A) := (\lambda_j(A^*A))^{1/2}. \tag{28}$$

Definition 3.2. [24, p. 59] *A compact linear operator A on a complex, separable Hilbert space $\mathcal{H}$ is called a trace class operator if*

$$\sum_j^{\nu(A)} \sigma_j(A) < \infty, \tag{29}$$

where $\nu(A)$ is the number of nonzero singular values of A. The collection of trace class operators on $\mathcal{H}$ is denoted by $\mathcal{J}_1(\mathcal{H})$.

The set $\mathcal{J}_1(\mathcal{H})$ endowed with the *trace class norm*

$$\|A\|_{\mathcal{J}_1} := \sum_j^{\nu(A)} \sigma_j(A), \quad A \in \mathcal{J}_1(\mathcal{H}), \tag{30}$$

is a two sided ideal [24, Thm. 5.1] of bounded linear operators on $\mathcal{H}$. Due to Weyl [41, Thm. 1.15], for a compact operator A on $\mathcal{H}$ we have

$$\sum_j |\lambda_j(A)| \leq \sum_j \sigma_j(A), \tag{31}$$

thus if $A \in \mathcal{J}_1(\mathcal{H})$,

$$\sum_j |\lambda_j(A)| < \infty. \tag{32}$$

Lemma 3.3. *L with kernel given by* (19) *is a trace-class operator on $L_2[0, 2\pi]$.*

Proof. Using the Bessel function asymptotic [39, 10.8.1], the leading non-analytic term in $L(t,s)$ is $O((t-s)^2 \log|t-s|)$ for small $t-s$, thus $L(t,s)$ and the partial derivative $\partial_s L(t,s)$ are continuous on $[0,2\pi]^2$, thus L is trace class on $L_2[0,2\pi]$ [18]. □

For trace-class operators, the Fredholm determinant as a linear functional can be constructed in several equivalent ways; we take the approach of Gohberg and Krein [25, p. 157]. For $A \in \mathcal{J}_1(\mathcal{H})$ with nonzero eigenvalues $\lambda_1(A), \lambda_2(A), \ldots$ (counting multiplicities), the Fredholm determinant of $I - A$ is defined by

$$\det(I - A) := \prod_{j=1}^{\infty} (I - \lambda_j(A)) \tag{33}$$

It is a well known result [30, p. 232] that (32) is equivalent to the absolute convergence of the right hand side of (33). An important property of the Fredholm determinant is that it completely describes when $I - A$ is invertible:

Theorem 3.4. [41, p. 34] *For $A \in \mathcal{J}_1(\mathcal{H})$, $\det(I-A) \neq 0$ if and only if $I - A$ is invertible.*

Corollary 3.5. *L with kernel given by* (19) *satisfies $\det(I - L) = 0$ if and only if $I - L$ has a nontrivial nullspace.*

Proof. The third Riesz theorem [20, p. 11] says if $I - L$ is not surjective, it is not injective. The claim then follows from Theorem 3.4. □

As we will see in Section 4, the nonzero eigenvalues of L will be approximated numerically by the nonzero eigenvalues of L_N in $C[0,2\pi]$. The following lemma connects those nonzero eigenvalues of L_N to the ones of the Nyström matrix, making accurate numerical approximation of $\det(I-L)$ possible.

Lemma 3.6. *The collection of nonzero eigenvalues, counting multiplicities, of L_N, defined in* (26)*, is the same as the nonzero eigenvalues of the associated Nyström matrix M_N as defined in* (27)*.*

Proof. It is well known that L_N and M_N have the same set of nonzero eigenvalues [33, Thm. 12.7]. We proceed to prove that each eigenvalue has the same multiplicity for L_N and M_N. If λ is a nonzero eigenvalue of L_N, then there exists a finite dimensional eigenspace with basis $\{\varphi_i\}$ such that $L_N\varphi_i = \lambda\varphi_i$ holds on $[0,2\pi]$. Certainly it holds on all the quadrature nodes, meaning $M[\varphi_i(s_k)]_{k=0}^{N-1} = \lambda[\varphi_i(s_k)]_{k=0}^{N-1}$, where $[\varphi_i(s_k)]_{k=0}^{N-1}$ indicates a column vector. It cannot be true that φ_i is simultaneously zero at all quadrature nodes, since then by (26), φ_i is identically zero on $[0,2\pi]$. By the same reasoning the set of $[\varphi_i(s_k)]_{k=0}^{N-1}$ for all i is a linearly independent set of eigenvectors of M_N with eigenvalue λ.

If on the other hand λ is a nonzero eigenvalue of M_N, then there exists a finite dimensional eigenspace with a basis spanned by the vectors $\{[\phi_{i,k}]_{k=0}^{N-1}\}$. For each i we can construct $\varphi_i(t) = \frac{1}{\lambda}\sum_{k=0}^{N-1}\{R_k^{(N)}(t)L^{(1)}(t,s_k) + \frac{2\pi}{N}L^{(2)}(t,s_k)\}\phi_{i,k}$, then $[\varphi_i(s_k)]_{k=0}^{N-1} = \frac{1}{\lambda}M_N[\phi_{i,k}]_{k=0}^{N-1} = [\phi_{i,k}]_{k=0}^{N-1}$. One sees that φ_i is an eigenfunction of L_N with eigenvalue λ, and $\{\varphi_i\}$ is a linearly independent set because the set $\{[\phi_{i,k}]_{k=0}^{N-1}\}$ is. □

The Fredholm determinant is a function of κ, and we use the notation (3) for the determinant of the exact operator. Similarly we use, for the matrix determinant of the associated Nyström matrix,

$$f_N(\kappa) := \det(I - M_N(\kappa)). \tag{34}$$

Remark 3.7. In fact, from Lemma 3.6, it follows that f_N is the Fredholm determinant of $I - L_N$ as a finite dimensional operator on $C[0, 2\pi]$. The definition of the Fredholm determinant for certain operators on a Banach space can be found in [24].

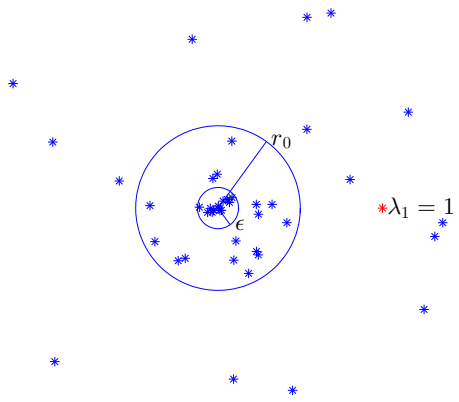

FIGURE 1. Illustration of proof idea for the main Theorem 4.3, showing spectrum of $L(\kappa_j)$, and circles of radius r_0 and ϵ.

4. Error analysis of the Fredholm determinant

We prove our main error analysis result in this section. The approximation sequence $\{L_N\}$ converges pointwise to the integral operator L on $C[0, 2\pi]$, and is collectively compact [33, p. 202]. The following two theorems of Atkinson describe the convergence of eigenvalues of L_N to the ones of L.

Theorem 4.1. [4] *Let K be an integral operator on a Banach space and $\{K_N\}$ be a collectively compact sequence of numerical integral operators approximating K pointwise, and let R and ϵ be arbitrary small positive numbers. Then there is an N_0 such that for $N \geq N_0$, any eigenvalue λ of K_N satisfying $|\lambda| \geq R$ is within ϵ of an eigenvalue λ_0 of K with $|\lambda_0| \geq R$. Furthermore let σ_N be the set of eigenvalues of K_N within distance ϵ from a fixed λ_0, then the sum of multiplicities of λ in σ_N equals the multiplicity of λ_0.*

To summarize, outside of an arbitrarily small disk eigenvalues of L_N approximate the eigenvalues of L with correct multiplicities. We also have the guarantee that the convergence rate of L_N is carried over to the eigenvalues.

Theorem 4.2. [5] *With the same assumption as in the above theorem, let λ_0 be of index ν, i.e., ν is the smallest integer for which*

$$\ker((\lambda_0 - K)^\nu) = \ker((\lambda_0 - K)^{\nu+1}), \tag{35}$$

where ker means the nullspace. Then for some $c > 0$ and all sufficiently large n,

$$|\lambda - \lambda_0| \leq c \max\{\|K\varphi_i - K_n\varphi_i\|^{\frac{1}{\nu}} \mid 1 \leq i \leq m\}, \tag{36}$$

for all $\lambda \in \sigma_n$, and the set $\{\varphi_1, ...\varphi_m\}$ is a basis for $\ker((\lambda_0 - K)^\nu)$.

When $\lambda_0 = 1$, then index is also called the Riesz number [20, p.11] of K. The Riesz number of our L is 1 [20, p. 84]. We can now prove the main theorem that the determinant of $I - M_N(\kappa)$ at an eigenfrequency $\kappa = \kappa_j$ vanishes exponentially with N.

Theorem 4.3. *Let κ_j^2 be a Dirichlet eigenvalue of a bounded domain Ω with analytic boundary. Then there exists an N_0 such that*

$$|f_N(\kappa_j)| \leq Ce^{-\alpha N}, \quad \text{for all } N > N_0, \tag{37}$$

where C and $\alpha > 0$ are constants depending on Ω and κ_j.

Remark 4.4. This theorem includes the case of Ω non-simply connected, although later we will show that a modification to the definition of $f(\kappa)$ and $f_N(\kappa)$ is needed to make a robust method for this case.

Proof. Let $\{\lambda_i^{(N)}\}_{i=1}^{N'}$ be the set of nonzero eigenvalues of $L_N(\kappa_j)$, counting multiplicities, where N' is at most N. Let $\{\lambda_i\}$ be nonzero eigenvalues of $L(\kappa_j)$. If κ_j is an eigenfrequency for (1)–(2), then according to Lemma 2.1, $I - L(\kappa_j)$ has nontrivial kernel. Based on Corollary 3.5, 1 is an eigenvalue of L, which we can label $\lambda_1 = 1$. Theorem 4.1 implies that we can pick an ordering of $\lambda_i^{(N)}$ so that $\{\lambda_1^{(N)}\}$ converges to λ_1 as $N \to \infty$, and there might be multiple such sequences, depending on the multiplicity of λ_1, i.e., essentially, the number of sequences with λ_1 as the limit is the same as the multiplicity of λ_1. We only need the existence of one such sequence for the following proof to hold. Theorem 4.1 also implies that if we let r_0 be a constant with $r_0 \leq \frac{1}{2}$, then there exists N_1 such that for $N \geq N_1$, the number of $\lambda_i^{(N)}$ with $|\lambda_i^{(N)}| \geq r_0$ equals the number of λ_i with $|\lambda_i| \geq r_0$, and we can relabel $\{\lambda_i^{(N)}\}_{i=1}^{N'}$ in such a way that $\lim_{N\to\infty} \lambda_i^{(N)} = \lambda_i$ for all i with $\lambda_i^{(N_1)} \geq r_0$.

Since by Lemma 3.6, $\{\lambda_i^{(N)} \mid 1 \leq i \leq N'\}$ is also the set of nonzero eigenvalues of $M_N(\kappa_j)$, we write the matrix determinant of $I - M_N(\kappa_j)$ as a product of three factors as follows,

$$\det(I - M_N(\kappa_j)) = \prod_{i=1}^{N'}(1-\lambda_i^{(N)}) = (1-\lambda_1^{(N)}) \prod_{|\lambda_i^{(N)}|\geq r_0,\ i\neq 1} (1-\lambda_i^{(N)}) \prod_{|\lambda_i^{(N)}|<r_0} (1-\lambda_i^{(N)}). \tag{38}$$

Then, for the second factor, since there are a finite number of terms,

$$\lim_{N\to\infty} \prod_{|\lambda_i^{(N)}|\geq r_0,\ i\neq 1} (1-\lambda_i^{(N)}) = \prod_{|\lambda_i^{(N)}|\geq r_0,\ i\neq 1} \lim_{N\to\infty} (1-\lambda_i^{(N)}) = \prod_{|\lambda_i|\geq r_0,\ i\neq 1} (1-\lambda_i). \tag{39}$$

Thus there exists N_2 and constant C_1 such that for $N \geq N_2$,

$$\left| \prod_{|\lambda_i^{(N)}|\geq r_0,\ i\neq 1} (1-\lambda_i^{(N)}) \right| \leq C_1.$$

For the third factor

$$\prod_{|\lambda_i^{(N)}|<r_0} |1-\lambda_i^{(N)}| \ = \ \exp\Big(\sum_{|\lambda_i^{(N)}|<r_0} \log|1-\lambda_i^{(N)}| \Big) \ \leq \ \exp\Big(\sum_{|\lambda_i^{(N)}|<r_0} 2|\lambda_i^{(N)}| \Big). \tag{40}$$

Choose $\epsilon \in (0, r_0)$, and let $m_N(\epsilon)$, $m_N(r_0)$ be the number of $\lambda_i^{(N)}$ with $|\lambda_i^{(N)}| \geq \epsilon$, $|\lambda_i^{(N)}| \geq r_0$, respectively; see Fig. 1. In Theorem 4.1, pick $R = \epsilon$, then there exists N_3 such that for $N \geq N_3$, all $\lambda_i^{(N)}$ with $|\lambda_i^{(N)}| \geq \epsilon$ are within distance ϵ of some λ_i, and each λ_i with $|\lambda_i| \geq \epsilon$ has exactly one

sequence $\{\lambda_i^{(N)}\}$ approaching it, i.e., we have $|\lambda_i^{(N)} - \lambda_i| < \epsilon$ and $|\lambda_i^{(N)}| \geq \epsilon$ for $N \geq N_3$. Then for $N \geq N_3$, we bound

$$\sum_{|\lambda_i^{(N)}|<r_0} |\lambda_i^{(N)}| = \sum_{|\lambda_i^{(N)}|<\epsilon} |\lambda_i^{(N)}| + \sum_{\epsilon\leq|\lambda_i^{(N)}|<r_0} |\lambda_i^{(N)}| \tag{41}$$

$$\leq (N' - m_N(\epsilon))\epsilon + \sum_{\epsilon\leq|\lambda_i|<r_0} |\lambda_i| + (m_N(\epsilon) - m_N(r_0))\epsilon \tag{42}$$

$$= (N' - m_N(r_0))\epsilon + \sum_{\epsilon\leq|\lambda_i|<r_0} |\lambda_i| \tag{43}$$

$$\leq N'\epsilon + \sum_{\epsilon\leq|\lambda_i|<r_0} |\lambda_i|, \tag{44}$$

where

$$\sum_{\epsilon\leq|\lambda_i|<r_0} |\lambda_i| \leq \sum_i |\lambda_i| \leq \|L(\kappa_j)\|_{\mathcal{J}_1},$$

which is bounded since by Lemma 3.3 L is in trace class.

For $\varphi \in \ker(I-L)$, from Lemma 2.3, φ is analytic, thus as discussed in Section 2.3, our quadrature scheme guarantees $\|L_N\varphi - L\varphi\|_\infty \leq Ce^{-a_0 N}$ for N sufficiently large, where $a_0 > 0$ and C are constants which only depend on φ. $\ker(I - L)$ is finite dimensional by Theorem 4.2, so there exists N_4, $a > 0$ and C_2 such that for $N \geq N_4$, $|1 - \lambda_1^{(N)}| \leq C_2 e^{-aN}$.

Let $N_0 = \max\{N_1, N_2, N_3, N_4\}$, then for $N \geq N_0$, since $N' \leq N$ we have

$$|\det(I - M_N(\kappa_j))| \;\leq\; C_2 e^{-aN} C_1 \exp(2N\epsilon + 2\|L(\kappa_j)\|_{\mathcal{J}_1}). \tag{45}$$

Now let $C := C_1 C_2 \exp(2\|L(\kappa_j)\|_{\mathcal{J}_1})$, then $|\det(I - M_N^{(\kappa_j)})| \leq Ce^{-(\alpha-2\epsilon)N}$, so we may choose any positive $\alpha < a - 2\epsilon$ to finish the proof. □

Remark 4.5. From the above proof, it is clear that when $\ker(I - L)$ is one-dimensional the rate α may be chosen arbitrarily close to a, the width of the strip in which the null-vector φ (density generating the eigenfunction) is analytic. A similar result holds for $\ker(I - L)$ higher-dimensional.

Remark 4.6. When the boundary Γ is merely C^∞ smooth (not necessarily analytic), we expect that $\ker(I - L)$ is in $C^\infty[0, 2\pi]$, and that the determinant converges to zero super-algebraically at eigenfrequencies. We leave a proof of this to future work.

Remark 4.7. Our numerical experiments suggest that the converse of Theorem 4.3 holds for simply-connected domains free from exterior resonances, in the sense to be discussed in Section 7. That is, if $f_N(\kappa_0)$ is numerically zero for sufficiently large N, κ_0 is a Dirichlet eigenfrequency.

5. Boyd's method for finding roots of the determinant

Here we describe a new approach to finding eigenvalues efficiently, using Theorem 3.4 to equate these with the roots of the Fredhold determinant $f(\kappa)$. Our method is inspired by the following fact.

Lemma 5.1. *$f(\kappa) = \det(I - L(\kappa))$ is analytic with respect to κ for $\kappa \in \mathbb{C}\backslash\{0\}$.*

Proof. For $L \in C[0,2\pi]^2$, $\det(I-L) = \sum_{m=0}^{\infty} \frac{(-1)^m}{m!} \int_0^{2\pi} ... \int_0^{2\pi} \det(L(t_p,t_q)_{p,q=1}^m) dt_1 ... dt_m$ [24, p. 112]. $L(t_p,t_q)$ is analytic in κ on $\mathbb{C}\backslash\{0\}$ by construction. Define $L_m := \det(L(t_p,t_q)_{p,q=1}^m)$ then L_m is analytic in κ on $\mathbb{C}\backslash\{0\}$. The idea is to show that $\det(I-L)$ is the uniform limit of the sequence of analytic functions $\{L_m\}$ on any compact set in $\mathbb{C}\backslash\{0\}$.

$$R_M := \left| \sum_{m=M}^{\infty} \frac{(-1)^m}{m!} \int_{[0,2\pi]^m} L_m(t_1,....,t_m) dt_1 ... dt_m \right| \tag{46}$$

$$\leq \sum_{m=M}^{\infty} \frac{1}{m!} (2\pi)^m \|L_m\|_{L^\infty} \tag{47}$$

$$\leq \sum_{m=M}^{\infty} \frac{1}{m!} m^{\frac{m}{2}} (2\pi \|L\|_{L^\infty})^m. \tag{48}$$

The second inequality comes from Hadamard's Inequality. As proved in [18], the power series $\Phi(z) = \sum_{m=1}^{\infty} \frac{m^{(m+2)/2}}{m!} z^m$ defines an entire function on $\mathbb{C}$, together with the fact that $\|L\|_{L_\infty}$ is uniformly continuous in κ on any compact set in $\mathbb{C}\backslash\{0\}$, we have $R_M \to 0$ as $M \to \infty$ locally uniformly in κ on $\mathbb{C}\backslash\{0\}$. Thus $\det(I-L)$ is the locally uniformly convergent limit of a sequence of analytic functions in κ on $\mathbb{C}\backslash\{0\}$. The claim follows. □

An analogous statement holds for our numerical approximation, namely that $f_N(\kappa)$ is analytic in κ close enough to the positive real axis. This follows from Lemma 3.6, which says $f_N(\kappa) = \det(I - M_N(\kappa))$, an N-dimensional matrix determinant, and the fact that matrix entries are linear combinations of Hankel functions. From Theorem 4.3, f_N vanishes exponentially fast at each eigefrequency κ_j, and thus, if we assume that the derivative $f_N'(\kappa_j)$ is bounded away from zero for sufficiently large N, the roots of f_N approach the true eigenfrequencies with accuracy exponential in N. When $f_N'(\kappa_j)$ is very small, as in the case of double or close roots, we switch to the SVD method as discussed in Section 8.

Remark 5.2. We do not prove that $f_N(\kappa)$ converges to $f(\kappa)$ exponentially for all κ; indeed the numerical evidence (Section 6) is that this convergence is merely algebraic for κ away from eigenfrequencies.

All that is now needed is an efficient method to find good approximations to the real roots of the numerical Fredholm determinant $f_N(\kappa)$. We propose Boyd's "degree-doubling" method [19], which, given that our function is analytic on the real axis, is spectrally accurate in the number of function evaluations [19]. Thus just a few evaluations per root found will be enough to approach machine accuracy.

Say we wish to find roots of f_N in an interval $\kappa \in [a,b]$. We change variable to $\kappa(\theta) = \frac{b+a}{2} + \frac{b-a}{2}\cos\theta$, choose a small number M, and evaluate the function on a regular grid in θ, i.e. $f_j = f_N(\kappa(\pi j/M))$, $j = 1, \dots 2M$. Note that only $M+1$ evaluations are needed since $\kappa(2\pi-\theta) = \kappa(\theta)$. Since $f_N(\kappa(\theta))$ is a 2π-periodic function of θ analytic in a neighborhood of the real axis, the Fourier representation

$$f_N(\kappa(\theta)) \approx \sum_{m=-M}^{M} c_m e^{im\theta} \tag{49}$$

is exponentially convergent in M. (This is equivalent to a Chebyshev expansion in the variable κ.) The coefficients $\{c_m\}$, being the discrete Fourier transform of the values f_j, are computed via the

fast Fourier transform of the vector $\{f_j\}$. In practice we start with $M = 4$, and double M, reusing previous f_j values, until $|c_M/c_0| \leq 10^{-12}$. Writing $z = e^{i\theta}$, (49) is a Laurent expansion in z, hence

$$q(z) \;:=\; z^M \sum_{m=-M}^{M} c_m z^m \tag{50}$$

is a degree-$2M$ Taylor series with the same nonzero roots. These roots are found by insertion of the vector $\{c_m\}$ into a companion matrix [23] and finding its eigenvalues μ_i at a cost of $O(M^3)$ (although we note that evaluation of f_j dominates over this cost by far). Finally, we fix a parameter ϵ and only the eigenvalues μ_i within ϵ of the unit circle are kept. In practice, we set ϵ to be 10^{-6} to capture close roots (whose effect is discussed in Section 8). We find that a smaller ϵ can lose one or more of the μ_i's. The kept μ_i's are converted back to give the roots $\kappa_i = \frac{b+a}{2} + \frac{b-a}{2} \operatorname{Re} \mu_i$. The imaginary parts

$$\beta_i := \frac{b-a}{2} \operatorname{Im} \mu_i \tag{51}$$

we observe to be good indicators of of the size of errors in the roots. This algorithm is available in `MPSpack` [11] as `@utils/intervalrootsboyd.m`

Finally, if the above criterion for Fourier series decay is not met with $M = 512$, or if it turns out that $|\beta_i| > \beta$, where β is a fixed algorithm error parameter, then the interval $[a, b]$ is instead subdivided and the process repeated on the smaller intervals.

6. Numerical results for a simply-connected domain

6.1. **Convergence of the Fredholm determinant.** To demonstrate the convergence of $f_N(\kappa)$ given by (34) as a function of N, the number of quadrature nodes on Γ, we use the non-symmetric planar domain described in Fig. 2. We test κ values near the 100th eigenfrequency κ_{100}. As the graph in Fig. 2 shows, for $\kappa = \kappa_{100}$, convergence to zero is at least exponential. However, as κ moves away from the eigenfrequency, the colorscale plot shows that the initial exponential convergence deteriorates to much slower algebraic convergence. We believe the latter is of third order, although we do not have a proof of this. (A possible explanation for third-order convergence is that it is what a naive Nyström method without Kress' analytic split would give for the operator $I - 2D$.)

6.2. **Convergence of the determinant roots to the eigenfrequencies.** With the same domain as above, we now verify the claim of the previous section that a simple root converges as fast as the rate of vanishing of the determinant at a true eigenfrequency. We solve for roots of $f_N(\kappa)$ on the interval $[20.4, 20.5]$ containing κ_{100} using the method of Section 5. Fig. 3 shows at least exponential convergence of the numerical root to its converged value κ_{100}. Note that 14-digit accuracy (15-digit relative accuracy) is achieved using only $N = 180$.

7. The resonance phenomenon and multiply-connected domains

7.1. **Spurious roots for domains with holes.** If the domain Ω has a hole, Theorem 2.2 does not apply, and we cannot therefore know that every root of the Fredholm determinant $f(\kappa)$ indicates a Dirichlet eigenfrequency of Ω. The following lemma characterizes this new scenario. We denote the inner boundary γ_1 and outer boundary γ_2. The normals on each boundary component of Ω point away from Ω. Also let Ω_i be the domain that γ_i encloses, where $i = 1, 2$; in particular $\Omega_2 = \Omega \cup \overline{\Omega_1}$. See Fig. 4(a).

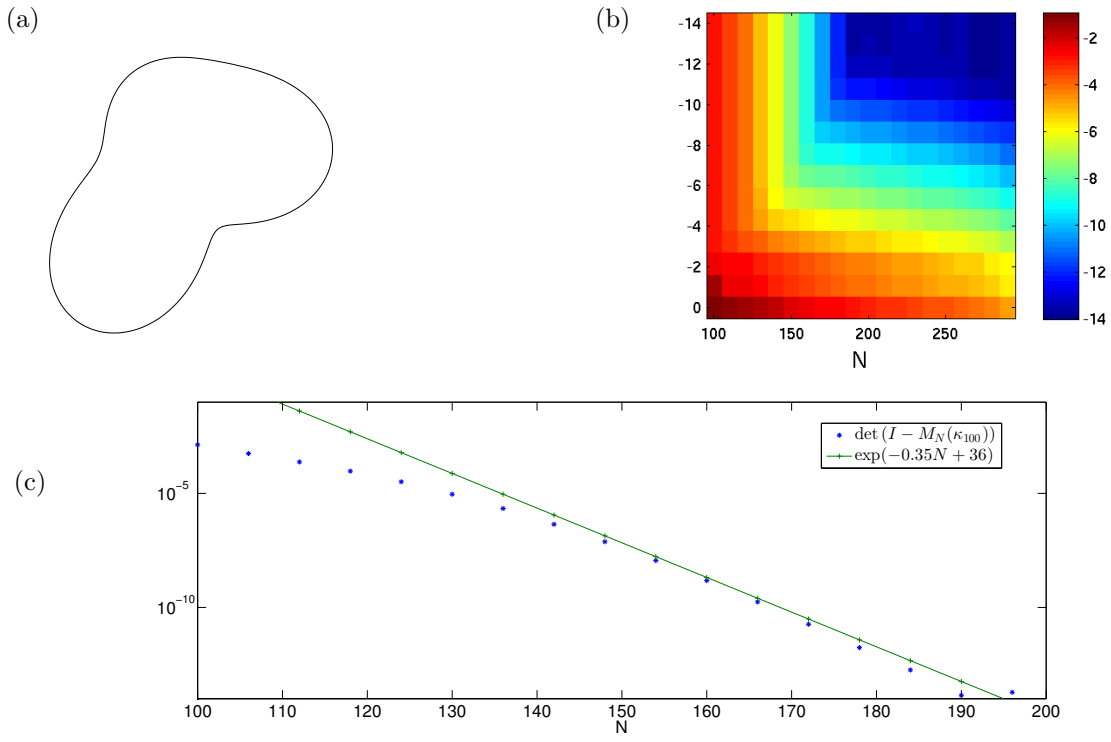

FIGURE 2. (a) Domain defined by $r(\theta) = 1 + 0.2\cos 3\theta + 0.3\sin 2\theta$. (b) $\log_{10} f_N(\kappa)$ near $\kappa_{100} = 20.43009417604$ (converged value); the vertical axis shows $\log_{10}(\kappa - \kappa_{100})$. (c) The convergence of $f_N(\kappa_{100})$ to zero, with N the number of quadrature nodes on the boundary. The line shows exponential convergence.

Lemma 7.1. *Let Ω be a domain with a hole Ω_1, and boundary $\Gamma = \gamma_1 \cup \gamma_2$. Then the operator $I - 2D(\kappa)$ on Γ has a nontrivial nullspace if κ is a Neumann eigenfrequency of Ω_1.*

Recall that Neumann eigenfrequencies are the discrete κ values where nontrivial solutions to (1) with $u_n = 0$ on Γ exist. Such eigenfrequencies generally do not coincide with the desired Dirichlet eigenfrequencies, thus our method of double layer potential produces incorrect roots for domains not simply connected. The obvious generalization of this lemma to domains with multiple holes also holds.

Proof. Ω_1 has countably many interior Neumann eigenmodes. For any such eigenmode with boundary data u and $u_n \equiv 0$ on γ_1, we can first extend u to $\tilde{u}$ defined on $\gamma_1 \cup \gamma_2$ by setting $\tilde{u} = 0$ on γ_2. We construct the double-layer potential $\mu := \mathcal{D}\tilde{u}$ at the corresponding eigenfrequency. Thus μ is a solution to the Helmholtz equation on $\mathbb{R}^2 \backslash \gamma_1$. Furthermore, for $x \in \mathbb{R}^2 \backslash \overline{\Omega_1}$, $\mu(x) = \mathcal{D}\tilde{u} = \mathcal{D}u = \mathcal{D}u - \mathcal{S}u_n = 0$ by Green's representation formula (17) applied to the exterior of Ω_1. Consider the continuous extension of μ from inside Ω to γ_1. From the jump relation (12), we see $(D - \frac{1}{2})\tilde{u} = 0$, i.e. the integral equation has a nontrivial solution. □

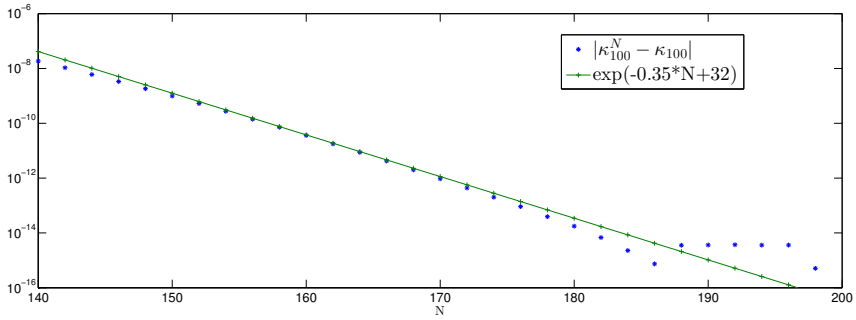

FIGURE 3. Convergence of the eigenfrequency error with N, the number of quadrature nodes on the boundary. The vertical axis shows the error (relative to its converged value) of the root found by the method of Sec. 5 at each N. The line shows exponential convergence.

(a)

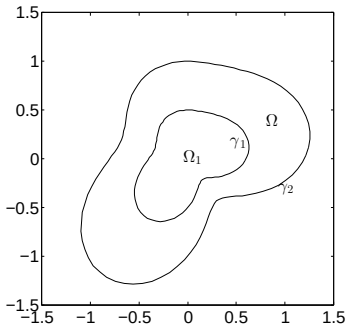

(b)

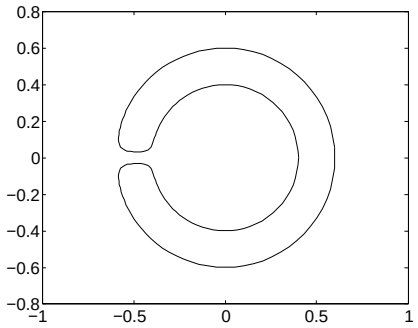

FIGURE 4. (a) Annular domain with boundary curves $\gamma_2 : r(\theta) = 1 + 0.2\cos 3\theta + 0.3\sin 2\theta$, and $\gamma_1 : r(\theta) = 0.5 + 0.1\cos 3\theta + 0.15\sin 2\theta$, $0 \le \theta \le 2\pi$; (b) Crescent-shaped domain with strong exterior resonances, with polar parametric description $r(s) = \frac{0.2}{1+\exp(4(s-3\pi/2)(s-\pi/2))} + 0.4$, $\theta(s) = -\frac{49}{50}\pi\sin s$, $0 \le s \le 2\pi$.

To summarize: for a domain with holes, if one solves for the roots of $f_N(\kappa)$, one gets not only the Dirichlet eigenfrequencies of Ω, but also the Neumann eigenfreqencies of the holes, which we call the *spurious roots*.

We now show that, on the real axis, this is the only failure mode of the pure double-layer representation. That is, the converse of the combination of Lemmas 2.1 and 7.1 also holds, as follows.

Lemma 7.2. *Let Ω be a domain with a hole Ω_1, boundary $\Gamma = \gamma_1 \cup \gamma_2$, and let $\kappa > 0$. If the operator $I - 2D(\kappa)$ on Γ has a nontrivial nullspace, then κ is either a Dirichlet eigenfrequency of Ω, or a Neumann eigenfrequency of Ω_1, or both.*

Proof. Let φ be a nontrivial function on Γ such that

$$(I - 2D(\kappa))\varphi = 0. \tag{52}$$

Let φ_i be the restriction of φ to γ_i, i.e. $\varphi_i = \varphi|_{\gamma_i}$ for $i = 1, 2$. Then φ_1 and φ_2 cannot be identically zero simultaneously.

Now let $\mu(x) := \mathcal{D}\varphi$, for $x \in \mathbb{R}^2 \backslash \Gamma$. If μ is not identically zero on Ω, we have constructed a Dirichlet eigenfunction on Ω by (52) and the jump relation (12). That is, κ is a Dirichlet eigenfrequency of Ω. If, however, $\mu \equiv 0$ on Ω, then $\mu_n^-(x) = 0$ for $x \in \gamma_2$. By the jump relation (13), $\mu_n^+(x) = \mu_n^-(x) = 0$ for $x \in \gamma_2$. On Ω_2, the exterior boundary value problem with zero Neumann boundary data has only the trivial solution [20, Thm. 3.13], so we have $\mu(x) \equiv 0$ for $x \in \mathbb{R}^2 \backslash \overline{\Omega}_2$. Thus $\mu^+(x) = 0$ for $x \in \gamma_2$. As a result, $\varphi_2 \equiv 0$ by (12), forcing $\varphi_1 \not\equiv 0$. In this case (52) reduces to $(I - 2D(\kappa))\varphi_1 = 0$, using the normal derivative pointing out of the annular domain Ω. Rewriting this using the usual normal pointing out of the simply-connected domain Ω_1, $(I + 2D(\kappa))\varphi_1 = 0$. Thus there is a Neumann eigenfunction on Ω_1 [20, Thm. 3.17] and κ is a Neumann eigenfrequency of Ω_1. □

The obvious generalization of Lemma 7.2 to multiple holes holds. The method of proof also applies to non-real κ, ruling out the Dirichlet and Neumann eigenfrequencies, but leaving the following variant.

Lemma 7.3. *Let Ω be a domain, not necessarily simply connected, with boundary Γ. Let $\kappa \in \mathbb{C}$, $\operatorname{Im}\kappa \neq 0$. If the operator $I - 2D(\kappa)$ on Γ has a nontrivial nullspace, the Neumann boundary value problem in the exterior component of Ω containing ∞ has non-unique solution, i.e. κ is an exterior Neumann resonance.*

Lemmas 7.1–7.3 completely characterize the roots of $\det(I - 2D(\kappa))$ in the complex plane for a domain Ω: all desired Dirichlet eigenfrequencies give roots, while Neumann eigenfrequencies of any holes in Ω and Neumann resonance of the exterior are the *only* mechanisms for producing spurious roots. They have an important consequence: even for a simply connected domain, as the geometry becomes sufficiently concave, spurious roots will show up numerically due to the exterior Neumann resonances (first observed in this context by Bäcker [8, Sec. 3.3.6]). The operator $I - 2D(\kappa)$ becomes singular for a $\operatorname{Im}\kappa$ very small and negative, resulting in a determinant very close to zero for a real κ. Any root-finding method working in finite precision thus may not distinguish those spurious roots from true eigenfrequencies. The severity of the issue is illustrated by the work of Betcke et al [16], where it is proved that for a cavity domain with an elliptical-shaped part, such resonances may exist with $|\operatorname{Im}\kappa|$ becoming *exponentially small* as $\operatorname{Re}\kappa$ grows.

We now demonstrate this problem, using the concave domain of Fig. 4(b). It closely resembles, and can be viewed as a smooth approximation of, an annular sector with inner radius 0.4, outer radius 0.6 and angular "openness" parameter $\frac{49}{50}\pi$. The disk with radius 0.4 has a Neumann eigenfrequency $\kappa_{\text{Neu}} = 26.2996521844$. And indeed, for the cresent domain, our root-finding method applied to $\det(I - 2D(\kappa))$ returns a spurious root $\kappa_0 = 26.30048303974$, clearly visible in Fig. 5(b). (This κ_0 is not exactly κ_{Neu} because the crescent domain is not an exact annulus.) We clarify that this spurious root does *not* disappear as N is increased; rather it converges to an exterior Neumann resonance with small imaginary part (in this case, around -10^{-7}).

7.2. **A new representation for the Dirichlet eigenvalue problem.** We can remedy the above non-robustness by constructing the boundary integral equation using the *combined field* potential,

$$u := \mathcal{D}\varphi + i\eta\mathcal{S}\varphi, \tag{53}$$

where η is a real parameter which, following [21], we set to be κ. This is standard in the acoustic scattering literature, but to our knowledge has not been used for the eigenvalue problem before. (The idea was suggested in one sentence of [8, Sec. 3.3.6].) Enforcing the Dirchlet boundary condition (2) on the combined field potential gives the CFIE

$$(I - 2D - 2i\eta S)\varphi = 0. \tag{54}$$

For the CFIE we have the following equivalence relation; in contrast to Theorem 2.2, it does not require simply connectedness of the domain.

Theorem 7.4. *Let Ω be a bounded domain with twice continuously differentiable boundary Γ. For each $\kappa \in \mathbb{C}\backslash\{0\}$ with $\operatorname{Im}\kappa \geq 0$, κ^2 is a Dirichlet eigenvalue of Ω if and only if $I - 2D(\kappa) - 2i\eta S(\kappa)$ has a nontrivial nullspace, where $\eta \neq 0$ is an arbitrary real number with $\eta \operatorname{Re}\kappa \geq 0$.*

Proof. "⇒" Suppose u is an eigenfunction, using the same argument as in Lemma 2.1 we have $(1-2D^T)u_n^- = 0$. Green's representation formula (17) says $Su_n^- = 0$. Thus $(1-2D^T-2i\eta S)u_n^- = 0$. In the dual system $\langle C(\Gamma), C(\Gamma)\rangle$ with the bilinear form $\langle\varphi,\psi\rangle := \int_\Gamma \varphi(x)\psi(x)dx$, S is self-adjoint and the adjoint of D is D^T [33, p. 41]. By the Fredholm alternative, $I-2D-2i\eta S$ has a nontrivial nullspace.

"⇐" Suppose $\varphi \in \operatorname{Null}(I-2D-2i\eta S)$ and φ is not identically zero. Consider $\mu := (\mathcal{D}+i\eta\mathcal{S})\varphi \in C^2(\mathbb{R}^2\backslash\Gamma)$, then μ satisfies (1) by construction. We look at $\mu^\pm$ and $\mu_n^\pm$ using the jump relations (10) through (13). First, μ satisfies the zero Dirichlet boundary condition for the interior problem since $\mu^- = (D - \frac{1}{2} + i\eta S)\varphi = 0$. So now we need only show that μ is nontrivial. Suppose μ is identically zero in Ω, then $\mu_n^- = [T + i\eta(D^T + \frac{1}{2})]\varphi = 0$. Thus we have $\mu^+ = (D + \frac{1}{2} + i\eta S)\varphi = \varphi$, and $\mu_n^+ = [T + i\eta(D^T - \frac{1}{2})]\varphi = -i\eta\varphi$. Therefore μ is a solution to (1) on Ω_+ with the impedance boundary condition

$$i\eta\mu + \mu_n \;=\; 0 \qquad \text{on} \quad \Gamma, \tag{55}$$

and μ is radiative in the exterior component containing infinity. In this infinite component μ has a unique solution when $\eta\operatorname{Re}\kappa \geq 0$ [20, p. 97], thus $\mu \equiv 0$ in this component. So φ must be identically zero on the boundary of this component. If Ω has no holes, we have reached a contradiction. Otherwise, let Ω_1 be any of the holes in Ω, with boundary γ_1. Let n' be the unit normal vector pointing to the exterior of Ω_1, then $n' = -n|_{\gamma_1}$. μ is a solution to (1) on Ω_1 with boundary condition

$$i\eta\mu - \mu_{n'} \;=\; 0 \qquad \text{on} \quad \gamma_1, \tag{56}$$

Multiplying each side of (1) by $\overline{\mu}$, integrating over Ω_1 and applying Green's first identity and (56), we get

$$\kappa^2\|\mu\|^2_{L^2(\Omega_1)} = \|\nabla\mu\|^2_{L^2(\Omega_1)} - i\eta\|\mu\|^2_{L^2(\gamma_1)}. \tag{57}$$

Taking the imaginary part we have $2\operatorname{Re}\kappa\operatorname{Im}\kappa\|\mu\|^2_{L^2(\Omega_1)} = -\eta\|\mu\|^2_{L^2(\gamma_1)}$, which is impossible given all the conditions on κ and η unless μ vanishes on γ_1. Hence $\mu_{n'}$ vanishes on γ_1 by (56). By Green's representation formula, μ is identically zero in Ω_1. We have shown $\mu \equiv 0$ in all of $\mathbb{R}^2\backslash\overline{\Omega}$ and this means φ is identically zero on Γ, which is a contradiction. So μ is a nontrivial solution to (1)–(2), hence an eigenfunction. □

Thus by adopting the combined field integral equation, we have a robust method with no spurious frequencies where the boundary operator is singular for κ real. We show this in Fig. 5, where we show the minimum singular value of (the Nyström approximation to) the original operator and of the CFIE, for (a) a doubly-connected domain and (b) a simply-connected domain with strong exterior resonances. In both cases this shows that the CFIE removes the spurious roots.

Remark 7.5. In order to eliminate the possibility of spurious roots for $\operatorname{Im}\kappa < 0$ numerically near the real axis, by analogy with Lemmas 7.2–7.3, one would need to show that (1) the interior Helmholtz impedance problem (with boundary condition (56)) for any holes in Ω, and (2) the radiative Helmholtz impedance problem in the infinite component exterior to Ω, both are resonance-free (have unique solution) for κ in some neighborhood of $\mathbb{R}$. Very recently (1) has been proven: there is a resonance-free strip lying below $\mathbb{R}$ for the interior impedance problem with an appropriate choice of η [14, Thm. 1.10]. However, we know of no result for the exterior problem. The numerical evidence in our study is that spurious roots do not occur near $\mathbb{R}$.

We now mention numerical implementation issues for the CFIE formulation.

For the spectrally-accurate discretization of the single-layer operator, we use the same method as for the double-layer, replacing L by $Q(t,s) = \Phi(x(t), x(s))|x'(s)|$, and replacing the logarithmically singular term (22) by [32, Eq. (2.6)]

$$Q^{(1)}(t,s) := -\frac{1}{2\pi} J_0(\kappa r(t,s)) \sqrt{x_1'(s)^2 + x_2'(s)^2}, \tag{58}$$

and defining $Q^{(2)}$ as before by the difference (23). Again with slight abuse of notation, we denote the integral operator Q and the Nyström matrix $Q_N(\kappa)$. For each N the determinant of the N-node Nyström discretization matrix $I - M_N(\kappa) - i\eta Q_N(\kappa)$ is analytic in κ. Thus we are able to apply the same root-finding method to it as before, and achieve rapid convergence with N for the roots, hence eigenvalues found.

Remark 7.6. We believe that the integral operator S is not a trace class operator, but could not find this in the literature. Certainly it is true for the Laplace case $\kappa = 0$ and Ω the unit disc, where S is a convolution operator with singular values $\sigma_j(S)$ decaying precisely as $1/j$ [33, Lemma 8.21]. For a general domain and $\kappa > 0$, S has pseudodifferential order -1, that is, $S : H^{-1/2}(\Gamma) \to H^{1/2}(\Gamma)$ is bounded [35, Thm. 6.11]. Thus its eigenvalues decay as $\lambda_j = O(1/j)$, according to [31, p. 192] by letting $p = q = 2$ and $\lambda = 1$. Since the integral kernel of S is symmetric, the eigenvalues of S are also the singular values $\sigma_j(S)$. If the asymptotic $\sigma_j(S) \sim c/j$ held as $j \to \infty$ then $\sum_j \sigma_j(S)$ would not converge, and for $\eta \neq 0$, $D + i\eta S$ would no longer be in $\mathcal{J}_1(L^2[0, 2\pi])$. Thus the main convergence Theorem 4.3 would not apply. However, we expect that numerically, Theorem 4.3 should be *close* to holding for the combined layer potential, since $\sum_j \sigma_j(S)$ can only diverge logarithmically. In addition, our experiments show that $\det(I - M_N(\kappa) - i\eta Q_N(\kappa))$ converges to zero as $N \to \infty$ if and only if $\kappa = \kappa_j$.

8. Close eigenfrequencies and the singular value method

Our root-finding method worsens in accuracy when $f(\kappa)$ has close roots, or roots with multiplicity higher than one. [1] In this section we discuss how we overcome this problem if it does occur, by reverting to the standard SVD method. Indeed, no method that relies on evaluating the Fredholm determinant $f(\kappa)$ alone could succeed in this case, because the root-finding problem is well known to

[1] Note that we do not expect this to occur too often, since for a generic domain eigenvalues are all simple [34].

(a)

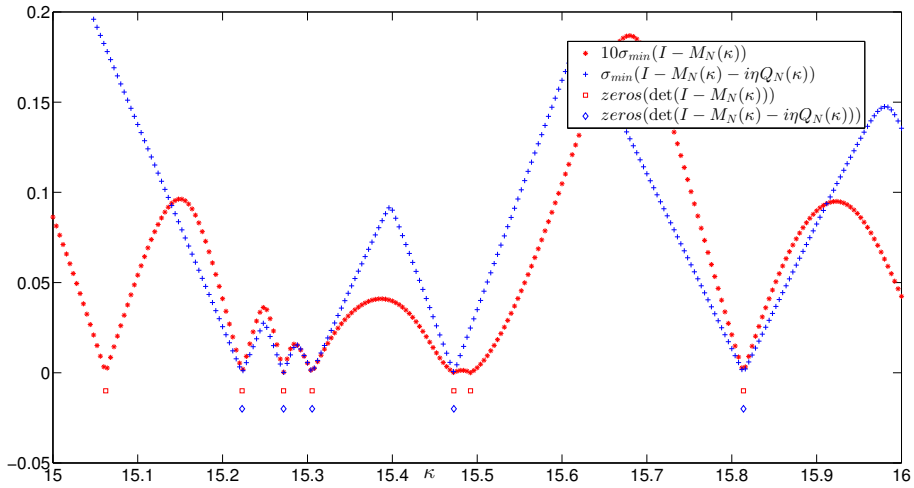

(b)

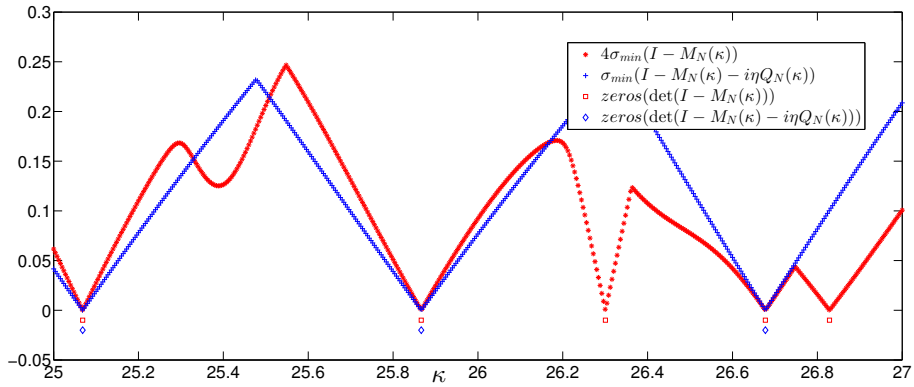

FIGURE 5. Lowest singular values vs frequency κ, for: (a) the annular domain Fig. 4(a); (b) the crescent domain Fig. 4(b). σ_{min} denotes the smallest singular value of the discretized $I - 2D(\kappa)$ (red), and CFIE $I - 2D(\kappa) - 2i\eta S(\kappa)$ (blue). The zeros of the corresponding determinants are shown by red squares and blue diamonds. The blue diamonds match the true eigenfrequencies. The number of quadrature nodes on the boundary is $N = 600$ (300 per curve component) in (a), and $N = 350$ in (b).

be ill-conditioned with respect to perturbations in the function (eg, for a polynomial, perturbations in its coefficients).

We discuss the case of two close eigenfrequencies $\kappa_j \approx \kappa_{j+1}$. Then $f(\kappa) = t(\kappa)(\kappa - \kappa_j)(\kappa - \kappa_{j+1})$ for some locally smooth function $t(\kappa)$. For simplicity, let f be perturbed by a constant value ε; then,

for small ε, the change induced in the root κ_j is of size

$$\delta\kappa \approx \left|\frac{\varepsilon}{f'(\kappa_j)}\right| = \left|\frac{\varepsilon}{(\kappa_{j+1}-\kappa_j)t(\kappa_j)}\right|, \tag{59}$$

which blows up inversely with the gap between the eigenfrequencies. This particular perturbation demonstrates the ill-conditioning; other perturbations lead generically to a similar effect. Even for $\varepsilon \approx 10^{-16}$ we may only retain accuracy $O(\varepsilon^{1/2})$ as two roots approach each other, and more if there are more close roots or a higher-order degeneracy.

To remedy this, when two roots are found closer than $s \approx 10^m\varepsilon$, where m is the desired number of digits of accuracy in rootfinding, we propose switching to a more expensive method based on the SVD. This requires finding the lowest singular values of the CFIE Nyström matrix $I - M_N(\kappa) - i\eta Q_N(\kappa)$, and is very similar to existing eigenvalue solvers [8, 15]. We only use the SVD when forced to do so since, due to the high cost of the SVD, and the increased number of function evaluations required to find each root, we will show that it is an order of magnitude less efficient than our proposed method.

Thus the choice of the parameter s affects the robustness and the speed of the algorithm. The smaller it is, the less often roots less than s apart will occur, and thus the faster the computation. However, smaller s causes a worsening of the accuracy of close roots. This is more severe for multiple roots: for $n > 1$, an order-n root has error on the order of $\varepsilon^{\frac{1}{n}}$, Thus to obtain desired accuracy, s has to be set to be large enough. In practice we fix $s = 10^{-3}$.

Once we switch to using the SVD on an interval of frequency κ, the smallest singular value $\sigma_{\min}(I - M_N(\kappa) - i\eta Q_N(\kappa))$ is far from analytic in κ (see Fig. 5 which shows the typical W-shaped function), so the Boyd's method is not useful. Instead we use recursive subdivision starting on a regular grid of values, followed by iterative parabolic fitting of $\sigma^2_{\min}(I - M_N(\kappa) - i\eta Q_N(\kappa))$ as detailed in [13, Appendix B]. This algorithm is available in `MPSpack` [11] as `@evp/gridminfit.m`

To demonstrate the higher accuracy of the SVD method over the Boyd's method in the presence of close eigenfrequencies, we choose an ellipse domain, and vary its eccentricity to cause a near-degeneracy of controllable separation $\kappa_{j+1} - \kappa_j$. Fig. 6 shows the eigenfrequencies passing through each other as a function of the eccentricity, solved by the determinant (red) and by the SVD methods (blue). Errors of absolute size around 10^{-7} appear in the determinant method but not the SVD method. As expected from (59), we see the errors $\delta\kappa$ blow up like $\frac{1}{|\kappa_{j+1}-\kappa_j|}$.

9. Numerical performance of the solver

In this section we demonstrate the improved efficiency of our solver, the Boyd's method with determinant, compared to an existing boundary-integral solver, namely the SVD method described in the previous section. We used a Linux workstation with two quad-core E5-2643 3.3GHz Xeon CPUs, running MATLAB R2013b, except for Hankel function evaluations which use Rokhlin's Fortran code `hank103.f` (eg see [11]).

9.1. **Non-resonant domain solved via pure double-layer representation.**

We computed the first 100 eigenfrequencies for the domain in Fig. 2(a) using both the Boyd's method and the standard SVD method as shown on the first two rows of table 1, respectively. For both methods, the initial number of quadrature nodes is scaled by setting $N = \max(150, 100 + 5\kappa)$. For the Boyd's method, the initial interval used was $[2, 5]$, converged $\kappa_{100} = 20.4300941760382$ and the largest N is 202. For moderate eigenfrequencies, as shown on the last two rows of table 1, we solved the 6 eigenfrequencies

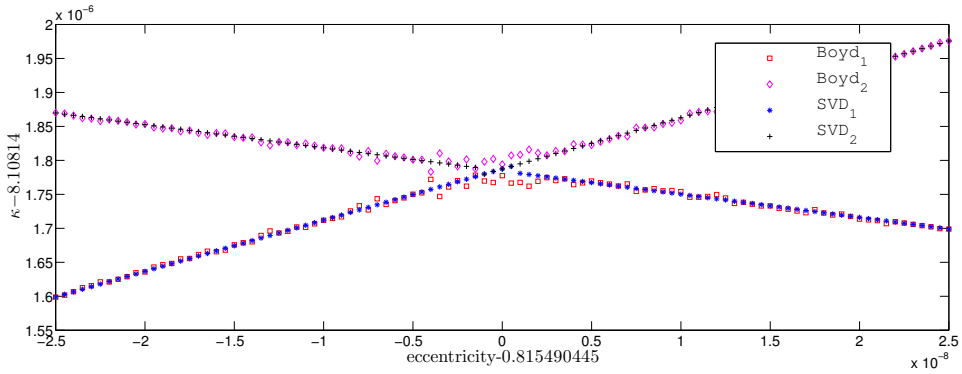

FIGURE 6. Two close eigenfrequencies of an ellipse crossing as a function of the eccentricity. Red shows values computed by Boyd's method applied to the determinant on the frequency interval $\kappa \in [7, 9]$. Blue shows values computed by the SVD method of Sec. 8. η is set to be zero since we expect and observe no exterior resonances.

in the interval $[100, 100.1]$ using 750 quadrature nodes using both methods. We used a pure double-layer potential ($\eta = 0$) since this domain is simply-connected and has no problem with exterior resonances. The error parameter from Section 5 is set to $\beta = 10^{-14}$.

For the Boyd's method, the error ϵ of each eigenfrequency is estimated using the magnitude of the imaginary part of the root found, as explained in Sec. 5. For the SVD method, error ϵ is estimated as follows. From Theorem 1 in [12], the distance of any fixed κ_0^2 to the true spectrum can be bounded by $C\kappa_0 t[u]$, where C is a constant depending only on Ω, u is a solution to (1) with $\kappa = \kappa_0$, and $t[u] := \|u\|_{L^2(\partial\Omega)}/\|u\|_{L^2(\Omega)}$ is a measure of the relative boundary error. Since our domain is star-shaped, we can use [12, (6.1)–(6.2)] to give an explicit estimate for C of approximately 3.5. By representing u as double layer potential with density φ, we have $u|_{\partial\Omega} = (D - \frac{1}{2})\varphi$ and $u|_\Omega = \mathcal{D}\varphi$. Numerically $t[u]$ can be bounded by $\frac{\sigma_{min}(I-M_N)}{2\|\mathcal{D}\hat{\varphi}\|_{L^2(\Omega)}}$, where $\hat{\varphi}$ is the associated right singular vector of $\sigma_{min}(I - M_N)$. Thus we estimate the relative error in κ to be $\frac{C\sigma_{min}(I-M_N)}{2\kappa\|\mathcal{D}\hat{\varphi}\|_{L^2(\Omega)}}$, where $\|\mathcal{D}\hat{\varphi}\|_{L^2(\Omega)}$ is estimated using crude quadrature scheme in the interior of Ω.

task	method	max Im $\tilde{\kappa}$	mean Im $\tilde{\kappa}$	max $\sigma_{\min}$	mean $\sigma_{\min}$	max ϵ	mean ϵ	Time (s)
$\kappa \leq 20.5$	Boyd's	7.3e-15	1.4e-15	1.7e-14	2.1e-15	3.8e-14	6.2e-15	20
	SVD	-	-	6.8e-11	1.6e-12	1.1e-10	2.6e-12	42
$\kappa \sim 100$	Boyd's	1.6e-15	7.4e-16	6.1e-15	3.2e-15	5.5e-14	3.3e-14	16
	SVD	-	-	3.1e-11	5.5e-12	1.1e-11	2.0e-12	151

TABLE 1. Performance data for the nonsymmetric domain in Fig. 2(a)

9.2. **Crescent-shaped domain solved via the CFIE.** For an example requiring the combined field potential for a robust solution, we test the highly-resonant crescent domain in Fig. 4(b). Computation is done again for the first 100 eigenfrequencies. In both methods, the number of quadrature nodes is given by $N = \max(350, 100 + 7\kappa)$. For the Boyd's method, the initial interval used was

[15, 17], converged $\kappa_{100} = 50.17535680154$ and the largest N is 456. The error parameter is set to $\beta = 10^{-12}$.

For error estimate, the C value for this highly concave domain is not known but we expect it to be $O(1)$ based on discussion in [12]. Thus we computed $\frac{\sigma_{min}(I-M_N-i\eta Q_N)}{2\|\mathcal{D}\hat{\varphi}\|_{L^2(\Omega)}}$, where $\hat{\varphi}$ is the associated right singular vector of $\sigma_{min}(I - M_N - i\eta Q_N)$, as an estimate for the relative error ϵ in κ, up to the constant factor C.

method	$\max \operatorname{Im} \tilde{\kappa}$	mean $\operatorname{Im} \tilde{\kappa}$	$\max \sigma_{\min}$	mean $\sigma_{\min}$	$\max \epsilon/C$	mean ϵ/C	Time (s)
Boyd's	6.7e-13	1.7e-14	4.9e-13	1.6e-14	2.1e-13	9.0e-15	98
SVD	-	-	3.5e-6	5.0e-8	1.4e-11	1.7e-13	368

TABLE 2. Performance data for the crescent domain in Fig. 4(b)

Remark 9.1. Boyd's rooting search method is sufficient to find the first 100 eigenfrequencies to at least 12 digits accuracy for those two examples, i.e., adjacent roots were never closer than 10^{-3} so the SVD was never needed to replace Boyd's method.

Remark 9.2. Typically, we find in the above experiments that Boyd's method requires around 5 function (determinant) evaluations per root found, while the SVD method needs around 15 (much more expensive) evaluations per root found. Note that it is possible to use a "sign-flipping" method to convert the minimum singular value function into an analytic function [17, sec. 9] for κ real. Thus it has recently been claimed that our determinant method has no advantage in terms of analyticity [2, Remark 6.4]. However, singular value plots such as Fig. 5, and those in [17, 2], show sudden bends in the function as it transitions from one V shape to the next, indicating a very small region of analyticity in κ that demands sufficiently dense sampling in an iterative root-finder. In contrast, Lemma 5.1 shows that the Fredholm determinant is analytic over essentially the entire complex plane, and is thus potentially more amenable to efficient (non-iterative) root-finding.

Finally, we show some eigenmodes of the crescent domain in Fig. 4(b), computed as follows. Once we obtain an eigenfrequency κ_j, we can extract the normal derivative data from the left kernel of the Nyström matrix $I - M_N(\kappa_j)$ then use Green's representation formula (17) to reconstruct the eigenmode. Fig. 7 shows the first 100 such modes; they are visually close to the separation-of-variable forms for an annular sector.

10. Conclusions

We have developed a robust method to compute Dirichlet eigenvalues for 2D domains with high accuracy and high efficiency compared to the traditional SVD root-finding method. We applied Boyd's root-finding method, exploiting the analyticity with respect to frequency of the Fredholm determinant of the boundary integral operator. This is approximated by the determinant of a Nyström matrix derived using as spectrally-accurate product quadrature. Since the determinant is cheap to evaluate, and Boyd's method requires only around 5 evaluations per eigenvalue found, we show that the method is 2-10 times faster than existing SVD-based methods.

In the case of an analytic boundary, we proved that our determinant has exponential convergence to zero at the true eigenvalues, and show that this rapid convergence carries over to the computed eigenvalues. Hence we are able to achieve 13 digits of relative accuracy for all eigenvalues computed for a star-shaped domain and 12 digits for a highly concave domain, with small numbers of boundary nodes. For multiply-connected domains or those with exterior resonances, we introduce a combined-field (CFIE) representation, prove that it is robust, and show that it eliminates spurious solutions

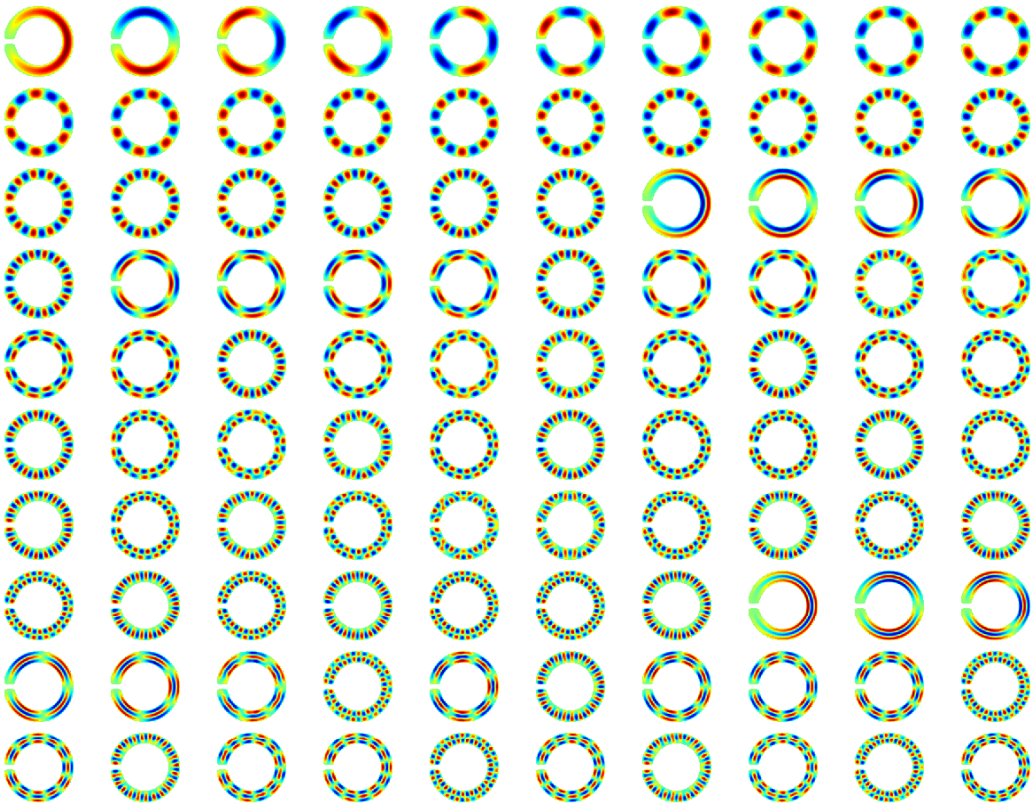

FIGURE 7. Modes u_1 to u_{100} of the crescent domain, computed via the CFIE method of this paper, as discussed in Sec. 9.

that are present in the standard approach. In the case of close eigenfrequencies, we revert to the SVD-based method; this is not a common occurrence.

We expect that corners, and thus very general domains, can be handled with a corner-refined quadrature scheme [32, 2]. One challenge remaining is to analyze a regularization of the CFIE (case $\eta > 0$) in which the Fredholm determinant is not infinite; the S operator we currently use in the CFIE we do not believe is in trace class (Remark 7.6). For this regularization we suggest considering $\mathcal{D} + i\eta\mathcal{S}^2$. Another theoretical challenge is to prove that the exterior impedance problem has a resonance-free strip (see Remark 7.5) which would rigorously exclude spurious roots in the CFIE with small negative imaginary part.

Finally, we note the recent introduction of an $O(N \log N)$ fast direct algorithm for the determinant of rank-structured matrices, such as the Nyström matrices appearing in this work, that opens up the possibility of fast version of the presented method when N is very large but the frequency κ is moderate [3].

Acknowledgments

The authors are grateful for the useful comments of the anonymous reviewers, for useful discussions with Euan Spence, and for support from the NSF under grant DMS-1216656.

References

[1] V. Akcelik, K. Ko, L. Q. Lee, Z. Li, and C. K. Ng. Shape determination for deformed electromagnetic cavities. *J. Comput. Phys.*, 227(3):1722–38, 2008.

[2] E. Akhmetgaliyev, O. Bruno, and N. Nigam. A boundary integral algorithm for the Laplace Dirichlet-Neumann mixed eigenvalue problem, 2014. `arxiv:1411.0071`.

[3] S. Ambikasaran and M. O'Neil. Fast symmetric factorization of hierarchical matrices with applications, 2014. `arXiv:1405.0223`.

[4] K. Atkinson. The numerical solution of the eigenvalue problem for compact integral operators. *Trans. Amer. Math. Soc.*, 129:458–465, 1967.

[5] K. Atkinson. Convergence rates for approximate eigenvalues of compact integral operators. *SIAM J. Numer. Anal.*, 12:213–222, 1975.

[6] I. M. Babuska and J. Osborn. Eigenvalue problems. In P. G. Ciarlet and J. I. Lions, editors, *Handbook of numerical analysis, Volume II*, pages 643–787. Elsevier (North-Holland), 1991.

[7] I. M. Babuska and S. A. Sauter. Is the pollution effect of the FEM avoidable for the Helmholtz equation considering high wave numbers? *SIAM J. Numer. Anal.*, 34(6):2392–2423, 1997.

[8] A. Bäcker. Numerical aspects of eigenvalue and eigenfunction computations for chaotic quantum systems. In *The mathematical aspects of quantum maps*, volume 618 of *Lecture Notes in Phys.*, pages 91–144. Springer, Berlin, 2003.

[9] A. H. Barnett. Asymptotic rate of quantum ergodicity in chaotic Euclidean billiards. *Comm. Pure Appl. Math.*, 59(10):1457–88, 2006.

[10] A. H. Barnett and T. Betcke. Quantum mushroom billiards. *CHAOS*, 17:043125, 2007.

[11] A. H. Barnett and T. Betcke. `MPSpack`: A MATLAB toolbox to solve Helmholtz PDE, wave scattering, and eigenvalue problems, 2008–2014. `http://code.google.com/p/mpspack`.

[12] A. H. Barnett and A. Hassell. Boundary quasi-orthogonality and sharp inclusion bounds for large Dirichlet eigenvalues. *SIAM J. Numer. Anal.*, 49:1046–1063, 2011.

[13] A. H. Barnett and A. Hassell. Fast computation of high frequency Dirichlet eigenmodes via the spectral flow of the interior Neumann-to-Dirichlet map. *Comm. Pure Appl. Math.*, 67(3):351–407, 2014.

[14] D. Baskin, E. Spence, and J. Wunsch. Sharp high-frequency estimates for the Helmholtz equation and applications to boundary integral equations, 2015. `arxiv:1505.01037`.

[15] T. Betcke. The generalized singular value decomposition and the Method of Particular Solutions. *SIAM J. Sci. Comp.*, 30:1278–1295, 2008.

[16] T. Betcke, S. N. Chandler-Wilde, I. G. Graham, S. Langdon, and M. Lindner. Condition number estimates for combined potential integral operators in acoustics and their boundary element discretisation. *Numer. Methods Partial Differential Equations*, 27:31–69, 2011.

[17] T. Betcke and L. N. Trefethen. Reviving the method of particular solutions. *SIAM Rev.*, 47(3):469–491, 2005.

[18] F. Bornemann. On the numerical evaluation of fredholm determinant. *Math. Comp.*, 79:871–915, 2010.

[19] J. P. Boyd. Computing zeros on a real interval through chebyshev expansion and polynomial rootfinding. *SIAM J. Numer. Anal.*, 40(5):1665–1682, 2002.

[20] D. Colton and R. Kress. *Integral equation methods in scattering theory*. Wiley, 1983.

[21] D. Colton and R. Kress. *Inverse acoustic and electromagnetic scattering theory*, volume 93 of *Applied Mathematical Sciences*. Springer-Verlag, Berlin, second edition, 1998.

[22] R. Courant and D. Hilbert. *Methods of mathematical physics. Vol. I*. Interscience Publishers, Inc., New York, N.Y., 1953.

[23] A. Edelman and H. Murakami. Polynomial roots from companion matrix eigenvalues. *Math. Comp.*, 64:763–776, 1995.

[24] I. Gohberg, S. Goldberg, and N. Krupnik. *Traces and Determinants of Linear Operators*. Birkhäuser, 2000.

[25] I. C. Gohberg and M. G. Krein. *Introduction to the theory of linear nonselfadjoint operators*. American Mathematical Society, Providence, 1969.

[26] D. S. Grebenkov and B.-T. Nguyen. Geometrical structure of Laplace eigenfunctions. *SIAM Review*, 53(4):601–667, 2013.

[27] P. Hähner. *Eindeutigkeits- und Regularitätssätze für Randwertprobleme bei der skalaren und vektoriellen Helmholtzgleichung*. Dissertation, Göttingen, 1990.
[28] S. Hao, A. H. Barnett, P. G. Martinsson, and P. Young. High-order accurate Nyström discretization of integral equations with weakly singular kernels on smooth curves in the plane. *Adv. Comput. Math.*, 40(1):245–272, 2014.
[29] S. M. Kirkup and S. Amini. Solution of the Helmholtz eigenvalue problem via the boundary element method. *Int. J. Numer. Meth. Eng.*, 36(2):321–330, 1993.
[30] K. Knopp. *Theorie and Anwendung der unendlichen Reihen*. Springer-Verlag, Berlin, 5th edition, 1964.
[31] H. König. *Eigenvalue Distribution of Compact Operators*. Operator Theory: Advances and Applications, volume 16. Springer Basel AG, 1986.
[32] R. Kress. Boundary integral equations in time-harmonic acoustic scattering. *Mathl. Comput. Modelling*, 15:229–243, 1991.
[33] R. Kress. *Linear Integral Equations*, volume 82 of *Appl. Math. Sci.* Springer, second edition, 1999.
[34] J. R. Kuttler and V. G. Sigillito. Eigenvalues of the Laplacian in two dimensions. *SIAM Rev.*, 26(2):163–193, 1984.
[35] W. C. H. McLean. *Strongly elliptic systems and boundary integral equations*. Cambridge University Press, 2000.
[36] M. Mitrea. Boundary value problems and Hardy spaces associated to the Helmholtz equation in Lipschitz domains. *J. Math. Anal. Appl.*, 202:819–842, 1996.
[37] K. Nakamura and T. Harayama. *Quantum Chaos and Quantum Dots*. Oxford Univ. Press, 2004.
[38] S. Nonnenmacher. Anatomy of quantum chaotic eigenstates. *Séminaire Poincaré*, XIV:177–220, 2010.
[39] F. W. J. Olver, D. W. Lozier, R. F. Boisvert, and C. W. Clark, editors. *NIST Handbook of Mathematical Functions*. Cambridge University Press, 2010. `http://dlmf.nist.gov`.
[40] N. Saito. Data analysis and representation on a general domain using eigenfunctions of Laplacian. *Applied and Computational Harmonic Analysis*, 25:68–97, 2008.
[41] B. Simon. *Trace Ideals and Their Applications*. American Mathematical Society, Providence, 2nd edition, 2005.
[42] L. N. Trefethen and T. Betcke. *Computed eigenmodes of planar regions*, volume 412 of *Contemp. Math.*, pages 297–314. Amer. Math. Soc., Providence, RI, 2006.
[43] H. E. Tureci and H. G. L. Schwefel. An efficient Fredholm method for calculation of highly excited states of billiards. *J. Phys. A*, 40:13869, 2007.
[44] H. E. Tureci, H. G. L. Schwefel, P. Jacquod, and A. D. Stone. Modes of wave-chaotic dielectric resonators. *Progress in Optics*, 47:75–137, 2005.
[45] G. Veble, T. Prosen, and M. Robnik. Expanded boundary integral method and chaotic time-reversal doublets in quantum billiards. *New J. Phys.*, 9:15, 2007.
[46] E. Vergini and M. Saraceno. Calculation by scaling of highly excited states of billiards. *Phys. Rev. E*, 52(3):2204–2207, 1995.

Department of Mathematics, Dartmouth College, Hanover, NH, 03755